Gain-Gratings and Dynamic Holography in Solid-State Laser Media

A. Brignon and J.-P. Huignard

Laboratoire Central de Recherches, Thomson-CSF, F—91404 Orsay, France

Optically written gain gratings in inverted laser media are investigated both theoretically and experimentally. We present a transient analysis, valid in the nanosecond-pulsed regime, that permits calculation of the diffraction efficiency and profile of the gain grating within the medium for both transmission- and reflection-type gratings. Because of the laser amplification experienced by all interacting beams, greater-than-unity diffraction efficiency is achievable. Application to high-speed dynamic holography is demonstrated in flash-lamp-pumped Nd:YAG and compact diode-pumped Nd:YVO_4 solid-state amplifiers.

Journal of Imaging Science and Technology 41: 474–481 (1997)

Introduction

Laser-induced gratings in dynamic media are suited for real-time holography.[1] Compared to photographic plates, the advantages of dynamic materials for holography are that no chemical processing of the recording medium is needed and dynamic holographic gratings follow the changes of the fringe pattern to be recorded. Applications of dynamic hologram recording include erasable holographic storage of information, real-time interferometry, and optical signal processing.[1] Optical phase conjugation by four-wave mixing (FWM) is another attractive application that permits correction of phase distorsions experienced by an optical wave when passing through an aberrating medium.

During the past, photorefractive materials have been extensively investigated for dynamic holography.[2–4] More recently, the mechanism of gain saturation in laser amplifiers was used to achieve wave mixing, real-time dynamic grating recording, and phase conjugation via FWM.[5–8] Phase conjugation was used to compensate the phase aberrations of laser media.[9,10] The use of solid-state laser amplifiers for such operations presents attractive features including automatic matching of nonlinearity with laser wavelength and high efficiency of the nonlinear process because of the laser amplification of all interacting beams. Thus, high diffraction efficiency has been demonstrated[11,12] in flash-lamp-pumped Nd^{3+}:YAG and diode-pumped Nd^{3+}:YVO_4 amplifiers[13] at the Nd:YAG laser fundamental wavelength ($\lambda = 1.06\ \mu m$). Because gain saturation is connected to stimulated laser emission, dynamic gain holograms can be written with very fast response times. As a first approximation, the response time is given by the dephasing time T_2 equal to a few picoseconds in Nd^{3+}-doped crystals.[14] After writing, gain holograms can be stored in a medium with a lifetime equal to the population lifetime τ of the upper laser level ($\tau \sim 100$ to $300\ \mu s$ in Nd^{3+}-doped crystals). Finally, inasmuch as gain saturation is inherent in all temporal regimes, dynamic holography and FWM in inverted media can be performed in both pulsed and cw regimes.[15,16]

Most theoretical analyses of gain-grating formation in distributed feedback lasers[17,18] and FWM interactions[6] has been in the steady-state regime. In this report we investigate the writing process of a single gain grating in a laser amplifier by two saturating coherent waves. To explain most of the experiments performed with nanosecond pulses delivered by *Q*-switched lasers, the modeling of this two-wave mixing interaction must be developed in the transient short-pulse regime. Such modeling is presented in Ref. 19 under the square pulse approximation of Ref. 20. More recently, modeling of transient FWM with orthogonally polarized pump beams and transient FWM with copolarized beams has been introduced.[12,16,21] These models are valid for arbitrary pump-beam energies of arbitrary temporal shapes. In this report, we present an exact formulation, readily obtained from these analyses, of the writing and reading processes of a single gain grating. This model permits calculation of the diffraction efficiency and prediction of the shape of the gain grating in the depth of the amplifier for both transmission- and reflection-type gratings. Influences of the absolute and relative energy densities of the writing pulses on diffraction efficiency are also described. Finally, we present dynamic holography experiments in a flash-lamp-pumped Nd:YAG amplifier and in a compact diode-pumped Nd:YVO_4 amplifier.

Gain-Grating Writing

The writing of a gain grating within a laser amplifier of length L is shown in Figs. 1(a) and 1(c) for both transmission- and reflection-type gratings, respectively. The two writing pulses of amplitudes A_1 and A_2 are provided by a separate Q-switched laser operating at a wavelength that sees maximum gain in the amplifier (on resonance operation). Writing beams A_1 and A_2 are assumed to enter the laser amplifier at time $t = 0$ and to have the same polarization. In the transmission configuration [Fig. 1(a)], the two writing beams enter the amplifier at the same

Original manuscript received December 9th, 1996.

E-mail: brignon@lcr.thomson.fr

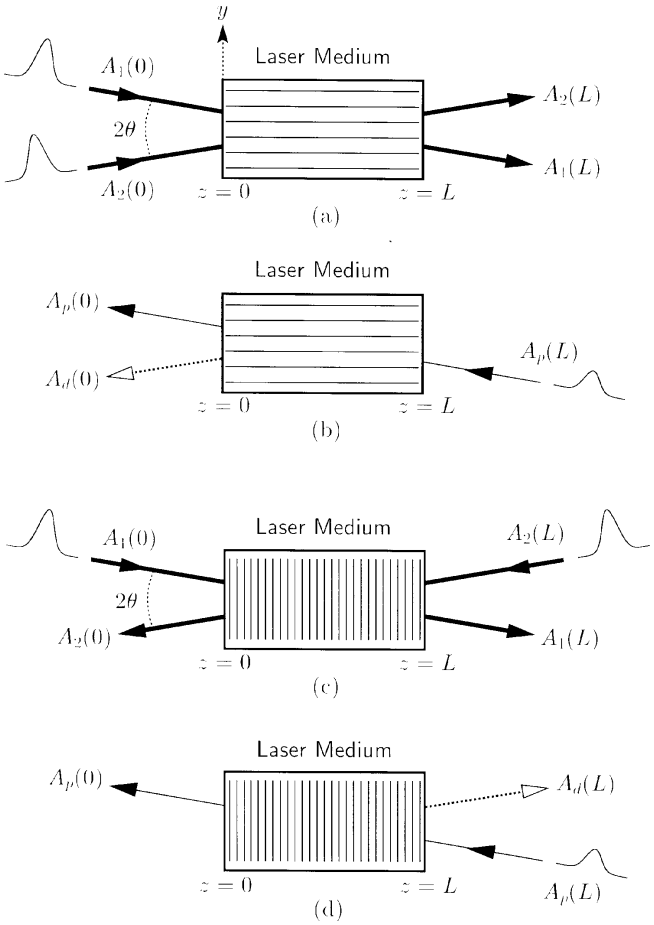

Figure 1. Schematic of (a) writing and (b) reading of a transmission-type gain grating by two coherent pulses in a laser amplifier, (c) writing and (d) reading of a reflection-type gain grating.

face ($z = 0$) and propagate along the z axis. The interferences of the two beams inside the amplifier produce periodic saturation of the gain that leads to a large-period gain grating. The half angle between the two beams is recognized as θ. In the reflection configuration [Fig. 1(c)], the two writing beams enter the amplifier at opposite faces and write a small-period grating. In this case, the half angle between the two beams is 90° – θ. The grating is written inside the medium and then stored during a time τ much longer than the duration t_p of the pulses (typically $t_p \sim 10$ ns and $\tau = 230$ μs in the case of Nd:YAG). It is then possible to read out the grating with a probe pulse of amplitude A_p at the same wavelength as the writing beams shown in Figs. 1(b) and 1(d) for the transmission and reflection configurations, respectively. The diffracted beam A_d is generated when the Bragg condition is fulfilled, i.e., when A_p is counterpropagating with respect to A_1. Note that the grating can be simultaneously written and read out. In this case the interaction is known as degenerate four-wave mixing (DFWM) and was analyzed in Refs. 12 and 16.

In the following theoretical analysis, we assume all the interacting beams are plane waves and that θ is small enough so all the field amplitude variations are along the z axis. We also assume the propagation duration in the medium is negligible relative to the pulse duration ($t_p >> n_0L/c$, where n_0 is the index of the medium and c is the speed of light). Under these approximations, the coupled equations, given the evolution of the writing beam intensities inside the gain medium at time t, can be readily deduced from Refs. 12 and 13:

$$\frac{dI_1(z,t)}{dz} = \alpha_0 \exp(-U_S)\left[I_0(U_M)I_1 - I_1(U_M)\sqrt{I_1I_2}\right], \tag{1a}$$

$$\in \frac{dI_2(z,t)}{dz} = \alpha_0 \exp(-U_S)\left[I_0(U_M)I_2 - I_1(U_M)\sqrt{I_1I_2}\right], \tag{1b}$$

where $\in = 1$ for the transmission configuration and –1 for the reflection configuration; I_1 and I_2 are the intensities of the writing beams A_1 and A_2, respectively; α_0 is the small-intensity gain coefficient, I_n ($n = 0,1$) is the n-th-order modified Bessel function; and

$$U_S(z,t) = \frac{1}{U_{sat}}\int_0^t (I_1 + I_2)dt, \tag{2a}$$

$$U_M(z,t) = \frac{2}{U_{sat}}\int_0^t \sqrt{I_1I_2}\,dt, \tag{2b}$$

where U_{sat} is the saturation fluence of the gain medium. Equations 1a and 1b can be numerically solved with the following boundary conditions: $I_1(0,t)$ = writing beam 1 in, $I_2(0,t)$ = writing beam 2 in, for the transmission configuration and $I_1(0,t)$ = writing beam 1 in, $I_2(L,t)$ = writing beam 2 in, for the reflection configuration. In this case, an iterative procedure is needed to solve Eqs. 1a and 1b because the boundary values of I_1 and I_2 are not both known at either end of the interaction region.[22] As shown in Ref. 23, resolution of Eqs. 1a and 1b permits calculation of the evolution of the gain grating profile inside the amplifier. After propagation of the two writing pulses ($t \geq t_p$), the spatially dependent gain coefficient g is given by

$$g(z) = \alpha_0 \exp\left[-U_S(z,t_p) - U_M(z,t_p) \times \cos\left(2\pi\frac{y}{\Lambda_T}\right)\right] \tag{3}$$

for the transmission configuration of Fig. 1(a), where $\Lambda_T \simeq \lambda/2\theta$ is the large grating period. Figure 2 shows the gain grating profile (Eq. 3) along the transverse axis y for various positions inside the medium ($z = 0$: input face; $z = L/2$: middle of the rod, and $z = L$: exit face). For clarity, we represented only four grating periods along the y axis. In these examples, a small-intensity gain-length product $\alpha_0 L = 4$ and a total input fluence $U_1(0) + U_2(0) = 0.1\ U_{sat}$ were assumed, where the fluence of beam A_j is defined as

$$U_j(z) = \int_0^{t_p} I_j(z,t)dt. \tag{4}$$

Curves of Fig. 2(a) were plotted for equal writing beam fluence, i.e., $\beta = U_1(0)/U_2(0) = 1$. In this case, $g = \alpha_0$ in the dark fringe region ($2y/\Lambda_T = 2n + 1$, n being an integer). The gain grating modulation depth is strongly dependent on the values of U_1 and U_2 relative to the saturation fluence U_{sat} of the gain medium. For this reason, when the values of $U_1(z)$ and $U_2(z)$ increase within the medium because of laser amplification, the gain-grating profile

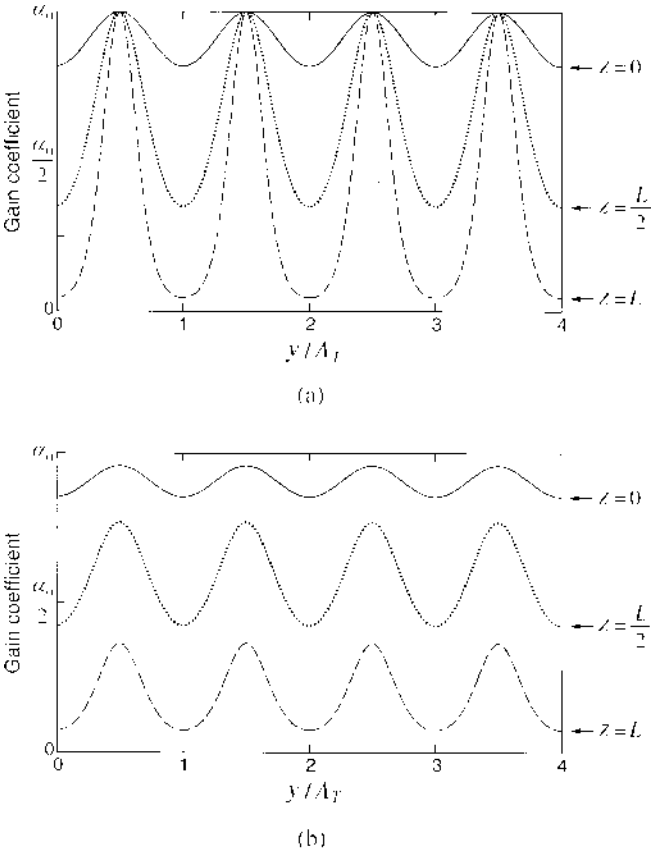

Figure 2. Gain coefficient obtained for a transmission-type grating as a function of the transverse axis y normalized to the grating period Λ_T, for various positions z, in the medium: (a) $\beta = U_1(0)/U_2(0) = 1$ and (b) $\beta = 10$. $\alpha_0 L = 4$; $U_1(0) + U_2(0) = 0.1 \times U_{sat}$.

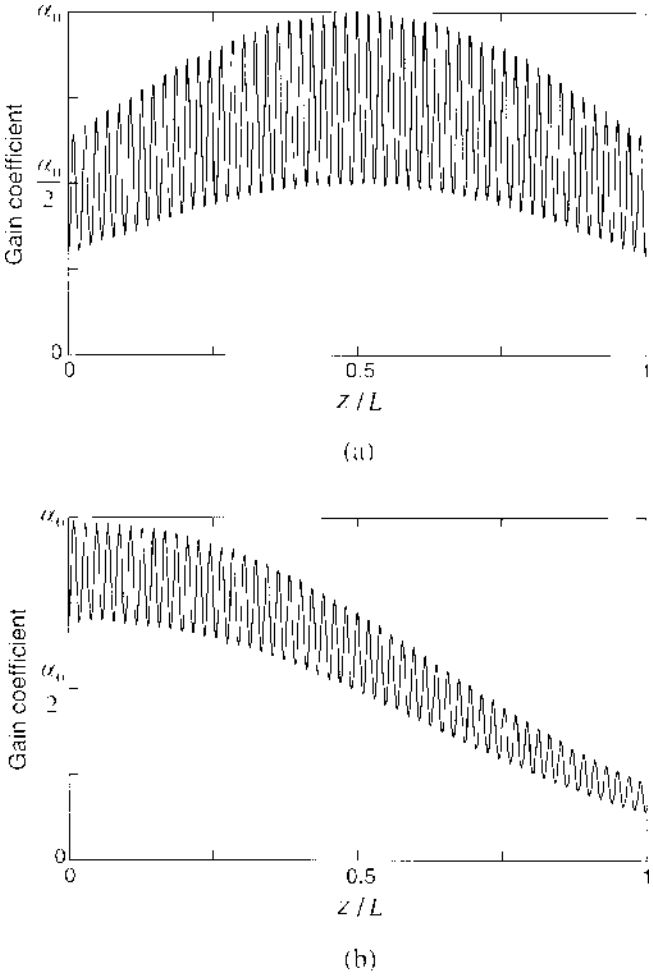

Figure 3. Gain coefficient obtained for a reflection-type grating as a function of the propagation axis z normalized to the length L of the medium: (a) $\beta = U_1(0)/U_2(L) = 1$ and (b) $\beta = 10$. $\alpha_0 L = 4$, $U_1(0) + U_2(L) = 0.1 \times U_{sat}$.

undergoes significant changes along the propagation z axis. Thus, at the input face, the gain grating has a low modulation depth and its profile is almost sinusoidal. But at the exit face, the gain grating has larger modulation and its profile is not sinusoidal as a result of the strong gain saturation in the bright fringe regions. Similar conclusions can be made for Fig. 2(b) curves plotted for $\beta = U_1(0)/U_2(0) = 10$. In this case, the intensity in the dark fringe regions is strong enough to saturate the gain, thus reducing the modulation depth of the gain grating as well as the total available gain.

Similarly, in the reflection configuration of Fig. 1(c), the spatially dependent gain coefficient g can be calculated as

$$g(z) = \alpha_0 \exp\left[-U_S(z,t_p) - U_M(z,t_p) \times \cos\left(2\pi \frac{z}{\Lambda_R}\right)\right], \tag{5}$$

where $\Lambda_R \simeq \lambda/2$ is the small-grating period. Figure 3 shows the gain-grating profile (Eq. 5) along the propagation axis z. For clarity, we represented only 50 grating periods along the z axis. As previously, a small-intensity gain-length product $a_0 L = 4$ and a total input fluence $U_1(0) + U_2(\mathrm{L}) = 0.1\ U_{sat}$ were assumed. For equal input writing beam fluence [$\beta = U_1(0)/U_2(L) = 1$], the envelope of the gain grating was symmetric relative to the middle of the medium at $z = L/2$ as shown in Fig. 3(a). At this position, the two writing beams had equal fluences, thus leading to a maximum modulation depth of the grating as well as a maximum gain in the dark fringe region ($g = \alpha_0$ for $2z/\Lambda_R = 2n + 1$, n being an integer). At both ends of the medium, minimum modulation depth and averaged gain were obtained because the two writing beams had different fluences. Indeed, in this case, only one writing beam experienced gain. For writing beams with different input fluences ($\beta \neq 1$), the gain-grating profile is not symmetric relative to the middle of the medium as shown in Fig. 3(b) [in this example, $\beta = U_1(0)/U_2(L) = 10$].

Diffraction Efficiency

After propagation of the writing beam inside the laser amplifier, the optically written gain grating can be read out by a probe beam to generate the diffracted beam. By assuming the probe pulse has a duration t_p and enters the medium at time $t = t_p$, the energy diffraction efficiency η of the gain grating can be expressed as

$$\eta = \frac{\int_{t_p}^{2t_p} I_d(0,t)dt}{\int_{t_p}^{2t_p} I_p(L,t)dt} \tag{6}$$

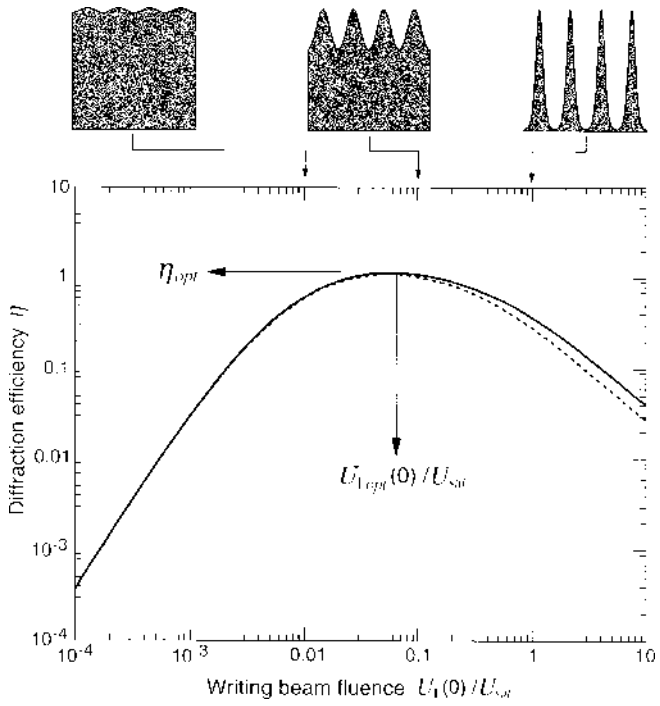

Figure 4. Energy diffraction efficiency versus writing beam fluence $U_1(0)$ normalized to the saturation fluence U_{sat} for transmission- (solid line) and reflection-type (dashed line) gain gratings. The three graphs above represent the gain grating profile (in the transmission geometry) at $z = 0$ for (from left to right) $U_1(0) = 0.01 \times U_{sat}$, $U_1(0) = 0.1 \times U_{sat}$, and, $U_1(0) = U_{sat}$. $\alpha_0 L = 4$, $\beta = 1$.

and as

$$\eta = \frac{\int_{t_p}^{2t_p} I_d(L,t)dt}{\int_{t_p}^{2t_p} I_p(L,t)dt} \tag{7}$$

for the transmission- and reflection-type gratings, respectively. The intensities of the probe and diffracted beams are I_p and I_d, respectively. To optimize the diffraction efficiency and to avoid additional saturation of the gain by the probe and the diffracted pulses,[19,12] we assume weak probe beam

The temporal integrals in Eqs. 6 and 7 are numerically calculated by solving the following set of equations at each time t:

(8a)

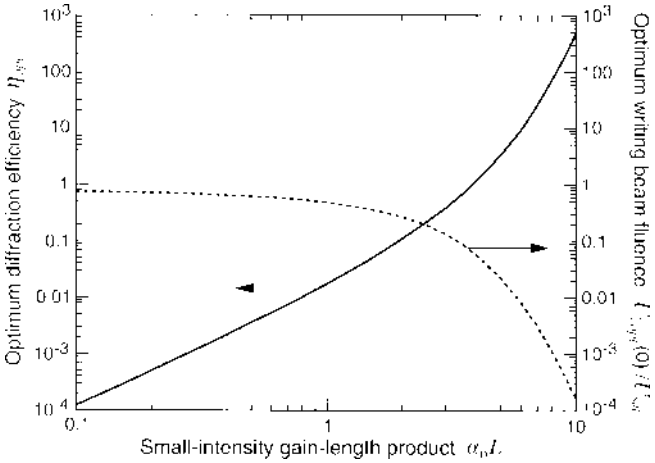

Figure 5. Optimum values of the diffraction efficiency (solid line) and writing beam fluence (dashed line) versus the small-intensity gain-length product $\alpha_0 L$. Transmission-type grating; $\beta = U_1(0)/U_2(L) = 1$.

(8b)

where U_S and U_M are given by Eqs. 2a and 2b and $\epsilon = 1$ for the transmission configuration and -1 for the reflection configuration. Equations 8a and 8b are subject to the following boundary conditions: $I_p(L,t)$ = probe beam in, $I_d(L,t) = 0$, for the transmission configuration and $I_p(L,t)$ = probe beam in, $I_d(0,t) = 0$, for the reflection configuration.

Figure 4 shows the diffraction efficiency η versus the writing beam fluence $U_1(0)$ for both transmission- and reflection-type gratings. In these examples, a small-intensity gain-length product $\alpha_0 L = 4$ and equal input writing beams ($\beta = 1$) were assumed. The diffraction efficiency rises at low writing beam fluence, reaches a peak value η_{opt} for an optimal value U_{1opt} of the writing beam fluence, and then falls for writing beam fluence above U_{1opt}. This behavior can be explained by observing the evolution of the gain-grating with the writing beam fluence. At low fluence [$U_1(0) \le 0.01 \times U_{sat}$], the modulation depth of the gain grating is very weak, thus leading to low diffraction efficiency as shown in Fig. 4. But in the high saturation regime [$U_1(0) \ge U_{sat}$], the modulation of the gain grating is strong but the gain is almost completely depleted in the bright fringe region. The optimum fluence value ($U_{1opt} \simeq 0.01 \times U_{sat}$) corresponds to a trade-off for achieving a noticeable modulation depth of the gain grating while having enough laser gain for efficient amplification of the diffracted beam. Note that transmission- and reflection-type grating curves behave the same. Both gratings also lead to a similar optimum diffraction efficiency $\eta_{opt} \simeq 110\%$, which shows that the grating period has almost no influence on the efficiency of the nonlinear process.

For practical applications, knowing η_{opt} and U_{1opt} is useful for a laser amplifier with a given small-intensity gain-length product $\alpha_0 L$. As shown in Fig. 5, η_{opt} increases while U_{1opt} decreases with $\alpha_0 L$. For weak gains,

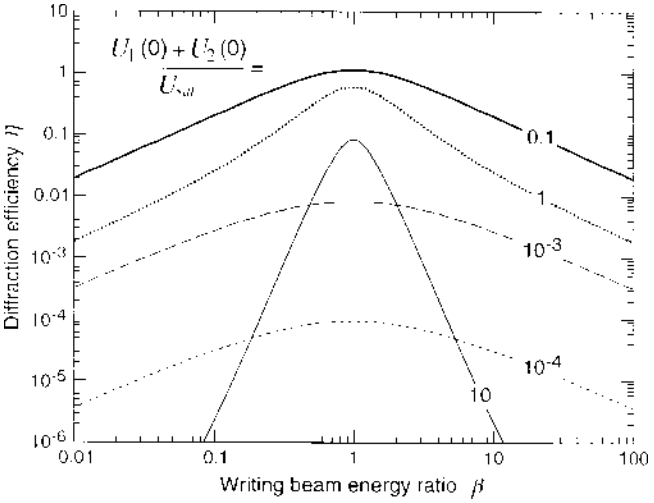

Figure 6. Energy diffraction efficiency versus the writing beam energy ratio $\beta = U_1(0)/U_2(0)$ for various values of the total writing beam fluence $U_1(0) + U_2(0)$. Transmission-type grating; $\alpha_0 L = 4$.

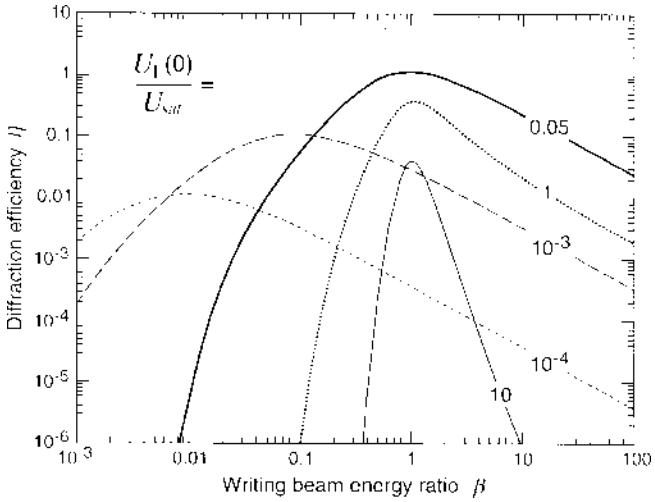

Figure 7. Energy diffraction efficiency versus writing beam energy ratio $\beta = U_1(0)/U_2(0)$ for various values of the writing beam fluence $U_1(0)$. Transmission-type grating; $\alpha_0 L = 4$.

optimum diffraction efficiencies are obtained for writing beam fluences equal to the saturation fluence $U_1 = U_2 \simeq U_{sat}$. Figure 5 also shows that for $\alpha_0 L > 3.8$, diffraction efficiencies greater than unity are achievable. The influence of the writing beam energy ratio $\beta = U_1(0)/U_2(0)$ (for the transmission geometry) on the diffraction efficiency is shown in Fig. 6 for various values of the total writing beam fluence $U_1(0) + U_2(0)$. Because the total writing beam fluence is fixed for each curve, the degree of saturation is independent of β. Variation of β only influences the contrast of the fringe pattern. As expected, optimum diffraction efficiency is thus obtained for $\beta = 1$, i.e., for maximum modulation depth of the gain grating. If the diffraction efficiency is plotted versus $\beta = U_1(0)/U_2(0)$ (transmission geometry) for a fixed value of $U_1(0)$, the curves of Fig. 7 are obtained. In this case, a variation of β influences both the degree of saturation and the contrast of the fringe pattern. For $U_1 \geq U_{1opt} \simeq 0.05 \times U_{sat}$, writing beam A_1 is strong enough to saturate the medium. In this case, only the contrast must be optimized and $\beta = 1$ for maximum diffraction efficiency. For $U_1 \leq U_{1opt}$, the trade-off between the degree of saturation and the contrast of the fringe pattern is obtained for $U_2(0) > U_1(0)$ ($\beta < 1$). For $U_1(0) = 10^{-4}\, U_{sat}$, maximum diffraction efficiency is thus obtained at $\beta \simeq 0.01$.

Recently, wave-mixing experiments were carried out in flash-lamp-pumped Nd:YAG amplifiers. In most of these experiments, the probe beam interacted simultaneously with the writing beams (DFWM experiments). With a conventional amplifier having a small-intensity gain-length product $\alpha_0 L \simeq 3 - 4$, gain-grating diffraction efficiencies between 20% and 50% were obtained.[11,12,19] Using a diode-pumped Nd:YVO_4 amplifier having a small-intensity gain-length product $\alpha_0 L = 1.2$, a diffraction efficiency of 6% has also been demonstrated. These experimental results are in good agreement with the transient modeling presented in Refs. 12 and 13.

Dynamic Holography in Laser Amplifiers

To demonstrate the ability of a conventional flash-lamp-pumped Nd:YAG amplifier for performing dynamic holography at $\lambda = 1.06$ μm, we conducted the experiment shown in Fig. 8. The laser rod had a length of $L = 11.5$ cm and a diameter of 7 mm. The two writing beams A_1 and A_2 were obtained from a single pulse of energy 15 mJ. This pulse of duration $t_p = 20$ ns was provided by a Q-switched TEM_{00}, 0.1-cm^{-1}-linewidth flash-lamp-pumped Nd:YAG oscillator. The oscillator and the amplifer were synchronized to ensure that the pulses experienced maximum gain in the amplifier. The small-intensity gain-length product was measured at $\alpha_0 L = 3.3$. A half-wave plate (WP_1) and Glan polarizer (GP) adjusted the writing beam ratio. The half-wave plate WP_2 allowed us to flip the polarization of A_1 to ensure that A_1 and A_2 have the same polarization. The writing beam A_2 was expanded by means of a diverging lens L_1 to illuminate a slide shown in Fig. 9(a). Writing beam A_2 was then focused inside the laser rod by lens L_2. To obtain good spatial overlap of the beams over the entire length of the Nd:YAG rod, the half angle between A_1 and A_2 was limited to $\theta \simeq 10$ mrad. The path lengths of the two beams were arranged to be equal at the center of the rod. The probe beam $A_p(L)$ was generated by reflecting the transmitted writing beam $A_1(L)$ with the mirror M_1 positioned at 15 cm from the end of the Nd:YAG crystal. To avoid saturation of the gain by the probe beam, a density (D) was used to attenuate $A_p(L)$. A beamsplitter (BS) was used to extract the diffracted beam. The reconstructed hologram was then monitored by means of a CCD camera as shown in Fig. 9(b). The quality of the reconstructed hologram was affected by the rod geometry of the amplifier that filters out the high spatial frequencies of the image. Nevertheless, this experiment shows, for the first time to our knowledge, that complex gain holograms can be recorded in conventional Nd:YAG amplifiers.

Recently, we showed that the diode-pumped Nd:YVO_4 amplifier was particularly adapted for applications to pulsed dynamic holography and wave-mixing interactions at the fundamental wavelength of neodymium lasers. Indeed, Nd:YVO_4 is a very efficient laser material that exhibits a large stimulated emission cross section as well as strong absorption at the diode laser pump wavelength. These factors combine to make Nd:YVO_4 particulary suitable for diode pumping.[24,26] Because the vanadate crystal and Nd:YAG have nearly identical spectral features, Nd:YVO_4 also can be used to amplify radiation from a Nd:YAG laser. Figure 10 shows the experimental setup for dynamic holography in a

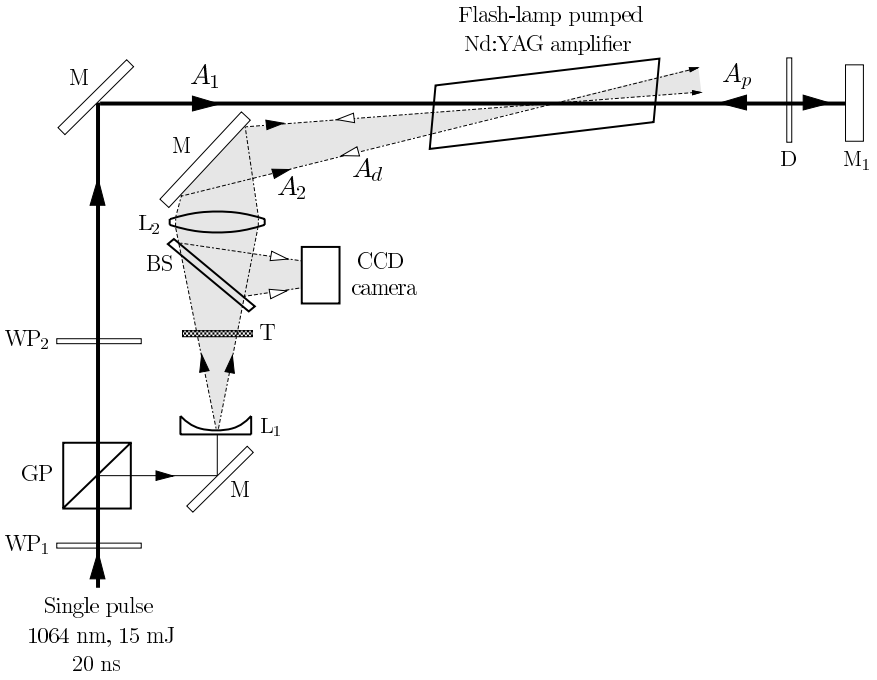

Figure 8. Experimental setup for pulsed dynamic holography at λ = 1.06 μm in a flash-lamp-pumped Nd:YAG amplifier. WP: half-wave plate; GP: Glan polarizer; M: high reflector; L: lens; T: transparancy (image); BS: beamsplitter; D: neutral density.

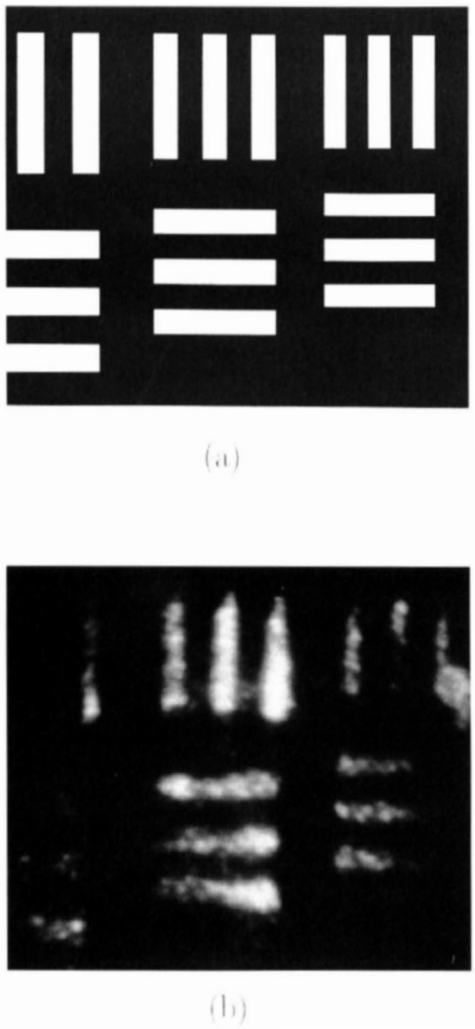

Figure 9. (a) Input image and (b) reconstructed hologram obtained in pulsed dynamic holography experiment in a flash-lamp-pumped Nd:YAG amplifier.

Nd:YVO_4 amplifier. The amplifier was a 1%-doped Nd:YVO_4 crystal with dimensions of 3 × 3 × 3 mm. Both a-cut end faces were polished flat and parallel. At the right face ($z = L$), the Nd:YVO_4 crystal was antireflection (AR) coated at the diode laser wavelength (809 nm) and high reflection (HR) coated at the wavelength to amplify (λ = 1.06 μm). The left side of the crystal ($z = 0$) was AR coated at λ = 1.06 μm. The amplifier was longitudinally pumped by a stack of four laser diode bars 10 mm long that produced 809-nm, 200-μs pulses at a power P = 130 W. About 80% of the diode laser beam was focused onto the crystal face ($z = L$) in a region of dimension 1.5 × 1.5 mm by means of a lens duct.[27] With such an amplifier, two-pass gain as high as 11 was demonstrated ($\alpha_0 L = 1.2$).

After 180 μs of diode pumping, the amplifier was almost in a state of maximum population inversion and the 20-ns writing pulses A_1 and A_2 at λ = 1.06 μm entered at the left side ($z = 0$) of the Nd:YVO_4 crystal as shown in Fig. 10. The two writing pulses were obtained from a single pulse delivered by a Q-switched, TEM_{00}, 0.1-cm^{-1}-linewidth Nd:YAG oscillator synchronized with the diode lasers. As previously, writing beam A_2 was expanded by means of a telescope to illuminate the image shown in Fig. 11(a). Writing beam A_2 was then refocused at about 2 cm behind the Nd:YVO_4 crystal. The small diameter of the incident image beam relative to that of the pump beams ensured that most of the image spatial frequency components interfered with the pump beams in the gain region. The gain hologram thus written in the inverted Nd:YVO_4 amplifier was simultaneously read out by the probe beam obtained by reflection of the transmitted writing beam $A_1(L)$ on the HR-coated face of the Nd:YVO_4 crystal. The reconstructed hologram is shown in Fig. 11(b) and 11(c). The diffraction efficiency of the dynamic holography device also can be controlled from pulse to pulse by varying the diode laser pumping power.[8]

Conclusion

Dynamic gain gratings, optically written in inverted laser media, were investigated. The use of solid-state laser amplifiers for such operations presents attractive features

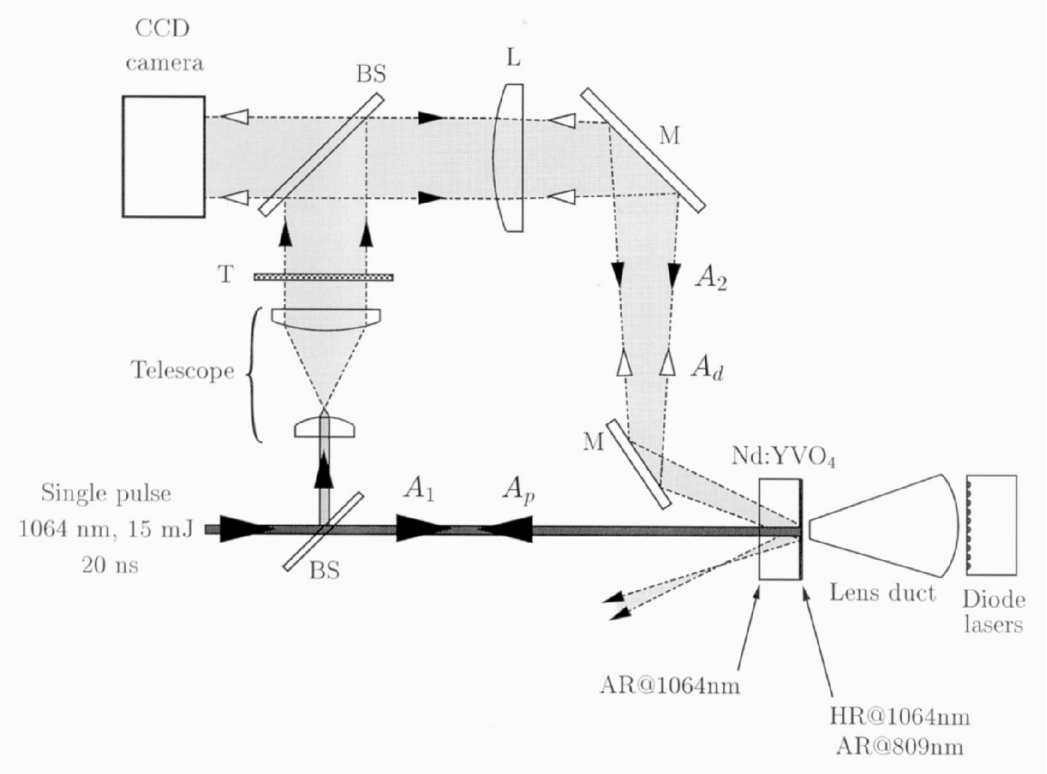

Figure 10. Experimental setup for pulsed dynamic holography at $\lambda = 1.06$ μm in a compact diode-pumped Nd:YVO$_4$ amplifier. BS: beamsplitter; L: lens; T: transparancy (image); M: high reflector.

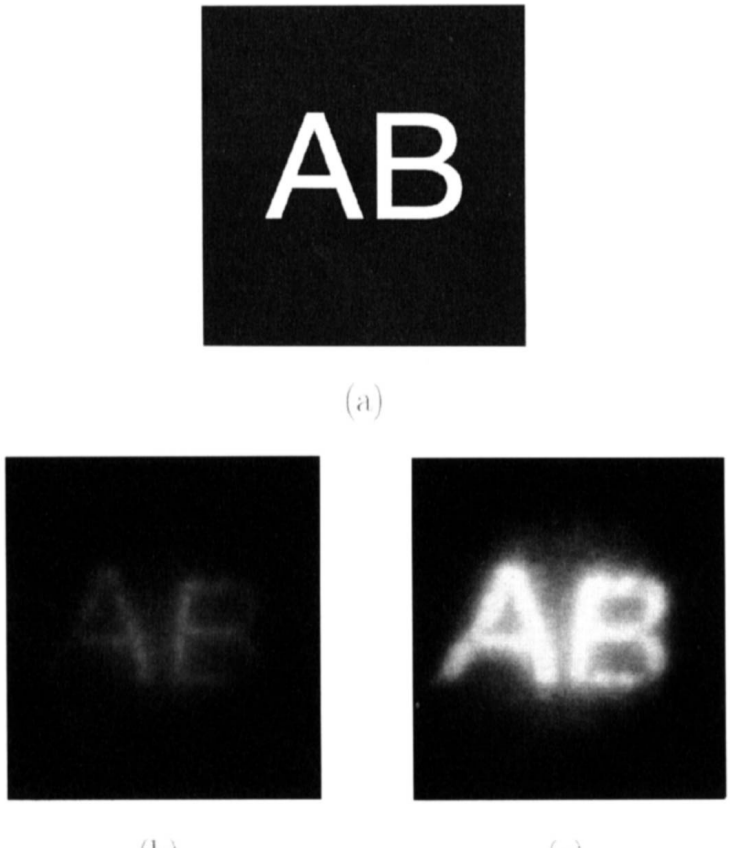

Figure 11. (a) Input image and (b) and (c) reconstructed hologram obtained in pulsed dynamic holography experiment in a compact diode-pumped Nd:YVO$_4$ amplifier. The efficiency of the gain hologram written in the Nd:YVO$_4$ amplifier was controlled by the diode laser pumping power P: (b) 50 W and (c) 100 W.

including automatic matching of nonlinearity with laser wavelength, fast response time, and high efficiency of the nonlinear process because of the laser amplification of all interacting beams. The gain grating or gain hologram is written inside the media and then stored for a time equal to the lifetime of the upper level of the laser transition. Read out of the grating with a probe pulse is then possible. We have presented a transient analysis, valid in the nanosecond-pulsed regime, that permits calculation of the energy diffraction efficiency and the profile of the gain grating within the medium for transmission- and reflection-type gratings. For both types of gratings, very similar diffraction efficiencies were calculated, which shows that the process of dynamic gain-grating recording is almost independent of grating period. This property is of great interest for dynamic holography because a large range of spatial frequencies can be recorded efficiently in contrast to other types of nonlinear media such as photorefractive materials. In addition, because of the laser amplification experienced by all interacting beams, greater-than-unity diffraction efficiency is achievable. The diffraction efficiency is strongly dependent on the energy ratio of the writing beams and on the input writing beam fluence relative to the saturation fluence of the gain media.

Dynamic holography experiments were conducted in flash-lamp-pumped Nd:YAG and compact diode-pumped Nd:YVO_4 solid-state amplifiers. In both cases, imaging capabilities of these devices were demonstrated. Thus, laser amplifiers appear to be a new class of promising nonlinear materials for application to high-speed dynamic holography and phase conjugation.

References

1. H. J. Eichler, P. Günter, and D. W. Pohl, *Laser-Induced Dynamic Gratings,* Springer-Verlag, Berlin, 1986.
2. J. P. Huignard and J. P. Herriau, Real-time double-exposure interferometry with $Bi_{12}SiO_{20}$ crystals in transverse electrooptic configuration, *Appl. Opt.* **16,** 1807–1809 (1977).
3. A. Marrakchi, J.-P. Huignard, and J. P. Herriau, Application of phase conjugation in $Bi_{12}SiO_{20}$ crystals to mode pattern visualization of diffuse vibrating structures, *Opt. Commun.* **34,** 15–18 (1980).
4. P. Günter and J.-P. Huignard, *Photorefractive Materials and Their Applications I and II*, Springer-Verlag, Berlin, 1989.
5. A. Tomita, Phase conjugation using gain saturation of a Nd:YAG laser, *Appl. Phys. Lett.* **34,** 463–464 (1979).
6. J. Reintjes, B. L. Wexler, N. Djeu, and J. L. Walsh, Degenerate frequency mixing in saturable amplifiers, *J. Phys.* (Paris) **44,** C2–27–C2–37 (1983).
7. G. J. Crofts, R. P. M. Green, and M. J. Damzen, Investigation of multipass geometries for efficient degenerate four-wave mixing in Nd:YAG, *Opt. Lett.* **17**, 920–922 (1992).
8. A. Brignon, G. Feugnet, J. P. Huignard, and J. P. Pocholle, Efficient degenerate four-wave mixing in a diode-pumped microchip Nd:$YV0_4$ amplifier, *Opt. Lett.* **20,** 548–550 (1995).
9. I. M. Bel'dyugin, V. A. Berenberg, A. E. Vasil'ev, I. V. Mochalov, V. M. Petnikova, G. T. Petrovskii, M. A. Kharchenko, and V. V. Shuvalov, Solid state lasers with self-pumped phase-conjugate mirrors in an active medium, *Sov. J. Quantum Electron.* **19,** 740–742 (1989).
10. R. P. M. Green, G. J. Crofts, and M. J. Damzen, Holographic laser resonators in Nd:YAG, *Opt. Lett.* **19,** 393–395 (1994).
11. R. P. M. Green, G. J. Crofts, and M. J. Damzen, Phase conjugate reflectivity and diffraction efficiency of gain gratings in Nd:YAG, *Opt. Commun.* **102,** 288–292 (1993).
12. A. Brignon and J. P. Huignard, Transient analysis of degenerate four-wave mixing with orthogonally polarized pump beams in a saturable Nd:YAG amplifier, *IEEE J. Quant. Electron.* **30,** 2203–2210 (1994).
13. A. Brignon, G. Feugnet, J. P. Huignard, and J. P. Pocholle, Multipass degenerate four-wave mixing in a diode-pumped Nd:$YV0_4$ amplifier, *J. Opt. Soc. Am. B* **12,** 1316–1325 (1995).
14. A. E. Siegman, *Lasers*, University Science Books, Mill Valley, California, 1986, chap. 8.
15. A. Brignon and J. P. Huignard, Continuous-wave operation of saturable-gain degenerate four-wave mixing in a Nd:$YV0_4$ amplifier, *Opt. Lett.* **20,** 2096–2098 (1995).
16. A. Brignon, Temporal analysis of pulsed phase conjugation in saturable amplifiers: application to Nd:YVO_4, *J. Opt. Soc. Am. B* **13,** 1748–1757 (1996).
17. M. Sargent III, Laser saturation grating phenomena, *Appl. Phys.* **9,** 127–141 (1976).
18. M. Sargent III, W. H. Swantner, and J. D. Thomas, Theory of distributed feedback laser, *IEEE J. Quant. Electron.* **QE-16,** 465–472 (1980).
19. A. Brignon and J. P. Huignard, Two-wave mixing in Nd:YAG by gain saturation, *Opt. Lett.* **18,** 1639–1641 (1993).
20. J. C. Diels, I. McMichael, and H. Vanherzeele, Degenerate four-wave mixing of picosecond pulses in the saturable amplification of a dye laser, *IEEE J. Quantum Electron.* **QE-20,** 630–636 (1984).
21. A. Brignon, J. Raffy, and J. P. Huignard, Transient degenerate four-wave mixing in a saturable Nd:YAG amplifier: effect of pump beam propagation, *Opt. Lett.* **19,** 865–867 (1994).
22. W. P. Brown, Absorption and depletion effects on degenerate four-wave mixing in homogeneously broadened absorbers, *J. Opt. Soc. Am.* **73,** 629–634 (1983).
23. A. Brignon and J. P. Huignard, Energy efficiency of phase conjugation by saturable-gain degenerate four-wave mixing in Nd:YAG amplifiers, *Opt. Commun.* **119,** 171–177 (1995).
24. J. E. Bernard and A. J. Alcock, High-efficiency diode-pumped Nd:YVO_4 slab laser, *Opt. Lett.* **18,** 968–970 (1993).
25. G. Feugnet, M. Schwarz, C. Larat, and J. P. Pocholle, TEM_{00} surface-emitting laser-diode longitudinally pumped Nd:YVO_4 laser, *Opt. Lett.* **18,** 2114–2116 (1993).
26. J. E. Bernard, E. McCullough, and A. J. Alcock, High gain, diode-pumped Nd:YVO_4 slab amplifier, *Opt. Commun.* **109,** 109–114 (1994).
27. G. Feugnet, C. Bussac, C. Larat, M. Schwarz, and J. P. Pocholle, High efficiency TEM_{00} Nd:YVO_4 laser longitudinally pumped by a high power array, *Opt. Lett.* **20,** 157–159 (1995).